



Spectroscopy of the shear force interaction in scanning near-field optical microscopy

Stefan Hoppe, Georgios Ctistis, Jens J. Paggel*, Paul Fumagalli

Freie Universität Berlin, Institut für Experimentalphysik, Arnimallee 14, 14195 Berlin, Germany

Received 24 February 2004; received in revised form 25 September 2004; accepted 12 October 2004

Abstract

Shear force detection is a common method of tip–sample distance control in scanning near-field optical microscopy. Shear force is the force acting on a laterally oscillating probe tip near a surface. Despite its frequent use, the nature of the interaction between tip and sample surface is a matter of debate. In order to investigate the problem, approach curves, i.e. amplitude and phase of the tip oscillation as a function of the tip–sample distance, are studied in terms of a harmonic oscillator model. The extracted force and damping constants are influenced by the substrate material. The character of the interaction ranges from elastic to dissipative. The interaction range is of atomic dimensions with a sharp onset. Between a metal-coated tip and a Cu sample, a power law for the force–distance curve is observed.

© 2004 Elsevier B.V. All rights reserved.

PACS: 68.37.Uv; 68.37.Ps; 68.35.Af

Keywords: Near-field optical microscopy (NFOM)

Scanning near-field optical microscopy (SNOM) is a technique combining atomic-force microscopy (AFM) with optical resolution beyond the diffraction limit [1]. The field of application for SNOM has spread in the last decade from physics into life science. This increased interest and the frequent use of this unique imaging technique calls for a

better understanding of the principal mode of operation. The fundamental ingredient for the imaging process is a suitable interaction between probe tip and sample to stabilize and control the tip–sample distance [2,3]. The distance-dependent shear force between a laterally oscillating optical-fiber tip and the sample is commonly used for this purpose [4,5]. The optical fiber is attached to a piezoelectric tuning fork, the tuning fork is excited and an electrical signal is extracted to measure the response. This signal is used by a feedback loop for distance control [6]. Most SNOMs operate with

*Corresponding author. Tel.: +49 30 83856095; fax: +49 30 83856299.

E-mail address: jens.paggel@physik.fu-berlin.de (J.J. Paggel).

this approach, but little is known about the origin of the involved forces. Some investigations in this field are made under ambient conditions [7–10] or low temperatures [11–13], and only a few under high [14] or ultra-high vacuum (UHV) [15] conditions. In recent years, the fundamental properties of the forces involved in tip–sample interaction were discussed by Refs. [16–19]. The forces observed in these investigations are due to fluctuating electromagnetic fields between tip and sample (van der Waals forces). They turn out to be much smaller than what is generally used for distance control in the SNOM. The discussion of the shear force interaction in the SNOM as presented here is thus at variance with the discussion in the later publications. Here the nature of the tip–sample interaction is analyzed under the conditions used for imaging. It will turn out that in this case, the tip is in mechanical contact with the sample. The use of samples with significantly different electronic properties (an insulator (SiO_x), a semiconductor (Si), and a metal (Cu)) yields access to the influence of the surface properties on the damping mechanism.

The experiments are performed under UHV conditions. Pressure during sample preparation was $<1 \times 10^{-10}$ mbar and $<1 \times 10^{-9}$ mbar during the experiments. All experiments were finished within less than 5 h after sample preparation. SiO_x is the native oxide on a silicon wafer. Prior to insertion into the vacuum system, the wafer was cleaned by successive rinsing in acetone, methanol, and purified water. Annealing the sample in vacuum to 650°C removed volatile contaminants. Clean $\text{Si}(111)-(7 \times 7)$ was prepared by heating the pre-cleaned Si-wafer to 1400°C . The Cu sample was a 100 nm Cu film grown on a clean SiO_x substrate in a different UHV chamber. After transfer through air, the Cu film was cleaned by Ar-ion sputtering. No C or O contamination was detectable by means of Auger-electron spectroscopy afterwards.

The oscillator system consists of a quartz tuning fork with an aluminum-coated (100 nm) fiber tip attached to one prong using a cyan-acrylate glue. The instrument operates in reflection mode. To avoid a shadowing of the reflected light by the tip itself, a long taper is needed. The tips used in our

instrument are therefore prepared by chemical etching in 40% hydrofluoric acid with a bromodecane protection layer. This recipe yields a cone angle of 29° [25]. A small apex angle directly converts to a long taper.

Fig. 1 shows the experimental setup in an equivalent-circuit diagram. The oscillator of a lock-in amplifier (LIA) (EG&G 7265) is used for excitation of the tuning fork. This excitation signal is connected through a voltage divider to one electrode. The second electrode is connected to a different LIA through a current-to-voltage converter [20]. This dual channel LIA (Femto LIA-BVD-150H) separates the real and imaginary part of the oscillation amplitude. These signals and the driving frequency are recorded by a computer. When excited, the tip moves laterally relative to the sample surface. The tip–sample interaction upon approaching the sample surface can cause a change in the damping constant $d_s(z)$ and in the force constant $k_s(z)$ as a function of the tip–sample distance z .

The mechanical oscillator is modeled by a driven harmonic oscillator. The electric response corresponds directly to the mechanical oscillation of the tuning fork [11]:

$$m \frac{\partial^2 x}{\partial t^2} + D \frac{\partial x}{\partial t} + Kx = Ae^{i\omega t}. \quad (1)$$

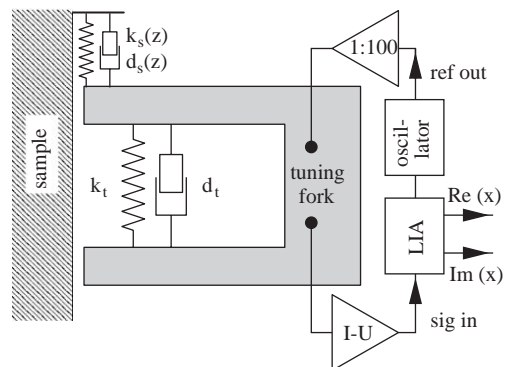


Fig. 1. Schematic diagram of the oscillator system. The tuning fork is modeled by a harmonic oscillator with force constant k_t and damping constant d_t . The interaction between sample and probe is approximated by $k_s(z)$ and $d_s(z)$ acting on one prong of the fork.

m represents the effective mass of the oscillating system, x denotes the lateral displacement of the tip, and ω is the driving frequency. The damping constant is $D(z) = d_s(z) + d_t$, and the force constant is $K(z) = k_s(z) + k_t$ as shown in Fig. 1.

Solving Eq. (1) yields the real and imaginary part of the amplitude x :

$$\Re(x) = \frac{A(K - m\omega^2)}{K^2 + \omega^2(D^2 - 2Km + m^2\omega^2)}, \quad (2)$$

$$\Im(x) = \frac{-AD\omega}{K^2 + \omega^2(D^2 - 2Km + m^2\omega^2)}. \quad (3)$$

From these, K and D are obtained:

$$D = \frac{A\Im(x)}{\omega(\Re^2(x) + \Im^2(x))}, \quad (4)$$

$$K = \frac{A\Re(x)}{\Re^2(x) + \Im^2(x)} + m\omega^2. \quad (5)$$

The real and imaginary part of the tip-oscillation amplitude are thus directly linked to the properties of the shear force interaction between tip and sample.

Fig. 2 shows a simulation (a) and three sets of experimental data (b–d). The simulation is

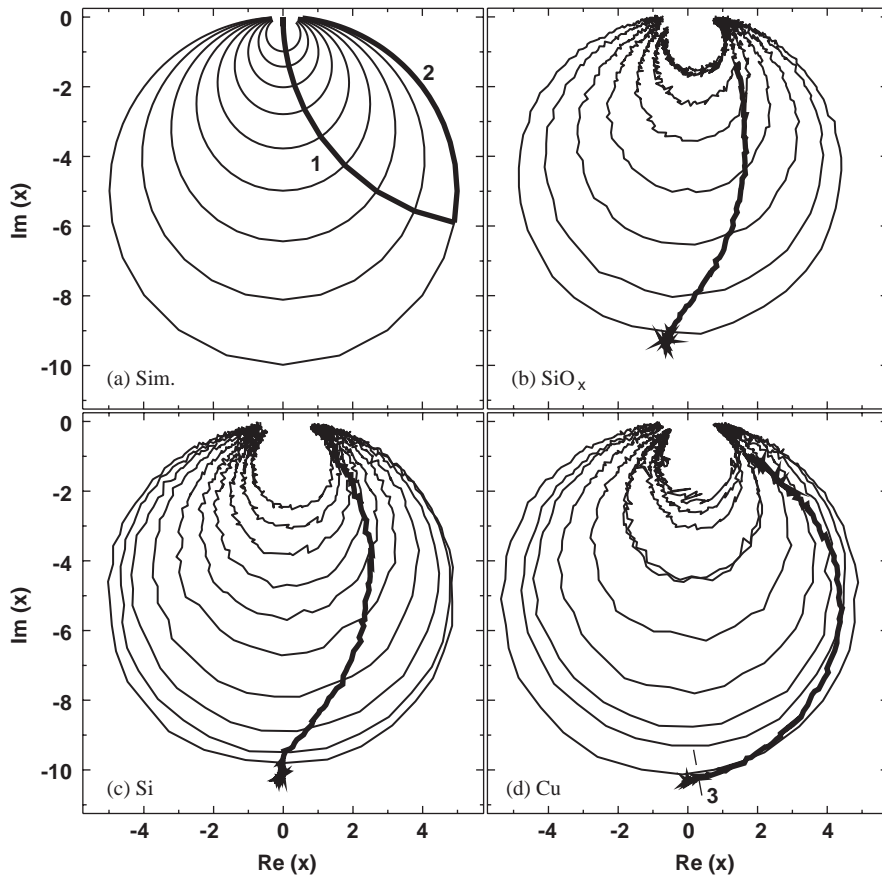


Fig. 2. (a) Simulation of harmonic oscillator amplitude plotted as imaginary vs. real part as a function of frequency (thin lines) for different damping constants. Sample traces (thick curves) of the resonance curves during approach for $K = \text{const.}$ (1) and $D = \text{const.}$ (2) Experimental approach and resonance curves plotted for SiO_x (b), Si (c), and Cu (d) surfaces.

used to discuss the principles of this unusual representation as imaginary vs. real part for the harmonic oscillator. Driving the oscillator through the resonance results in circles. The circles are called resonance curves. Increasing the damping constant reduces the oscillation amplitude and results in smaller circles. When the oscillator frequency is fixed and the tip-sample distance is changed, the distance-dependent interaction between tip and sample will modify amplitude and phase of the tip motion. These curves are called approach curves. We usually observe a hysteresis between tip approach and retraction, indicating a mechanical contact between tip and sample, that modifies the interaction (or the probe tip). We restrict the discussion to approach curves.

Curves (1) and (2) in Fig. 2(a) are simulated examples. In the case of an entirely dissipative interaction between tip and sample, the curve crosses the circles at right angle (1). When the interaction is elastic, the curve follows a circle (2). Eq. (1) is used to describe the approach curves in a quantitative way [6,21]. The motion of the tuning fork is however in principle that of a bending beam and not a simple harmonic oscillator. Thus an equivalent mass and equivalent spring constant are calculated as follows. The tuning fork has an eigenfrequency of $\nu_0 = 32\,768$ Hz. One prong is $L_r = 3.9$ mm long, $t_r = 600$ μm thick, and $w_r = 330$ μm wide. The optical fiber is attached to one prong, so half of its cross-sectional area has to be added to the cross-section of the prong ($t = 617$ μm). The elastic constant of quartz is $E = 8.68 \times 10^{10}$ N/m² and its density is $\rho = 2649$ kg/m³ [24]. In order to arrive at an eigenfrequency close to the experimentally observed one, a length of $L = 4115$ μm for the prong has to be used. The slightly larger length of the prong accounts for a number of inadequacies, such as the possible influence of the anisotropy of the elastic constants of quartz and the details of the influence of the finite thickness of the base of the tuning fork on its oscillation frequency. It however demonstrates that attaching the tip to the prong imposes only a minor modification to the oscillator. A basic discussion of the properties of tuning forks can be found in Ref. [22]. The resonance frequency

is computed according to [23]

$$\nu_0 = \frac{1.875^2 t}{2\pi L^2} \sqrt{\frac{E}{12\rho}} = 33\,690 \text{ Hz.} \quad (6)$$

The measured eigenfrequency of the tuning fork is $\nu_m = 33\,513$ Hz. The spring constant and the equivalent mass in the equivalent harmonic oscillator then follow as

$$k_t = \frac{1}{4} E w_r \left(\frac{t}{L}\right)^3 = 24\,139 \frac{\text{N}}{\text{m}}, \quad (7)$$

$$m = \frac{k_t}{\omega_m^2} = \frac{24\,139 \text{ N/m}}{(2\pi 33\,513 \text{ 1/s})^2} = 5.4 \times 10^{-7} \text{ kg.} \quad (8)$$

The excitation force as last unknown parameter is obtained from the static deflection of the oscillator:

$$A = k_t \Re(\omega \ll \omega_{\text{resonance}}). \quad (9)$$

With these parameters absolute scales may now be used for the graphs of the damping and force constants vs. distance. The motion of the tuning fork itself is not approximated by a harmonic oscillator.

Figs. 2(b)–(d) show experimental resonance and approach curves for the different materials. Fig. 2(b) shows the experiment for SiO_x. The approach curve crosses the resonance curves at about 45°, indicating a combination of dissipative and elastic interaction. Si [Fig. 2(c)] as a semiconducting material behaves similar to the insulator. The experiment for Cu is shown in Fig. 2(d). The interaction starts mainly elastic. For smaller tip-sample distances, the approach curve crosses the smaller circles, indicating the onset of a dissipative interaction.

In Fig. 3 force and damping constants extracted from the approach curves are plotted vs. tip-sample position on a linear scale in the left column. The right column shows the background-subtracted curves in a logarithmic plot. Zero on the distance scale is chosen arbitrarily. For SiO_x and Si, the maximum value of the damping constant is 20–30% larger than for Cu. The force constants are more similar, indicating that the observed force constant likely originates from the probe tip. All parameters are on the same order of magnitude. One interesting common feature of all curves is the

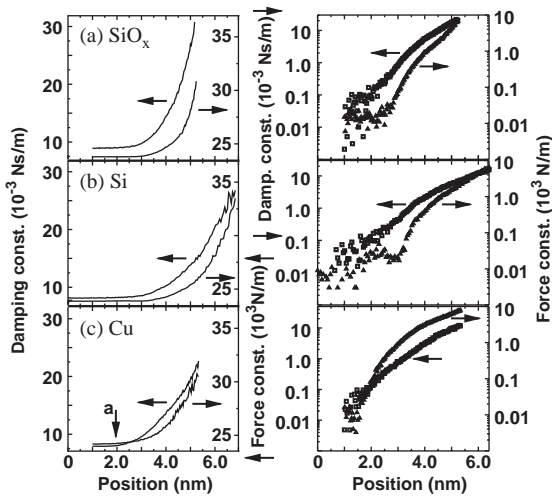


Fig. 3. Force and damping constant plotted for SiO_x (a), Si (b), and Cu (c) surfaces on a linear scale (left column) and logarithmic scale (right column). Left scales in the columns are background subtracted damping constants; right scales correspond to force constants.

short range of the interaction. The turn-on of the interaction is sharp, apparently much sharper than in the experiment by Karrai and Tiemann [14]. For Cu, the change in force and damping constant starts simultaneously. For Si and SiO_x the dissipative interaction starts well before the elastic interaction.

The sharp onset and the finite range of the interaction of a few nanometer does not immediately render electrostatic or electrodynamic forces as cause of the shear force interaction between tip and sample unlikely. A power law would indicate an interaction in the realm of classical physics, an exponential behavior a quantum mechanic origin. Clearly none of the traces follows a simple exponential dependence.

To check for a power law, a double-logarithmic plot is necessary. This requires a precise determination of the origin on the distance axis. A simple way to find this point to a precision of a few angstroms is to measure the electrical resistance between a metal-covered tip and a conductive sample as a function of distance. We are interested in the point of contact. A small bias voltage is thus mandatory, otherwise the tip will be destroyed upon contact. The experiment, with an applied

bias voltage of 100 mV on the Cu sample, puts the point of contact exactly to the onset of observed tip–sample interaction (marked by the arrow ‘a’ in Fig. 3 and the thin line (3) in Fig. 2). The error of this distance is on the order of a few angstroms. Both polarities for the bias voltage are used in the experiment. The result was not influenced by the chosen polarity of the voltage. It is thus shown without doubt that the change in force and damping constant at the level relevant for SNOM starts for a metal-coated tip in front of a Cu surface at mechanical contact. The shear force interaction as applied to SNOM is thus a variety of the contact atomic-force microscopy experiments.

Using this distance calibration, we analyze the force–distance curves in a double-logarithmic plot [Fig. 4(a)]. The plot is linear and thus a power law for the force–distance characteristic is observed. The corresponding power is 3.8. The dissipative

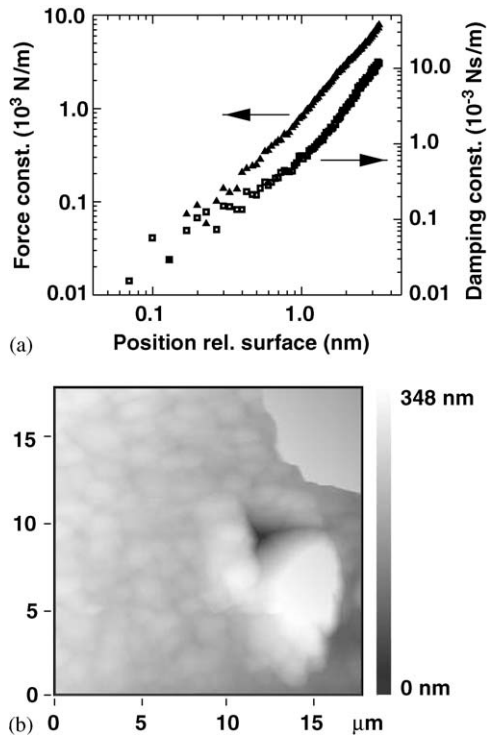


Fig. 4. (a) Force and damping constant for the approach curves to the Cu surface in a double-logarithmic representation. (b) Topographic image showing the point of contact for the approach curves.

part of the interaction is shown along with the elastic part and does not follow a power law. The destructive nature of the tip–sample interaction in our approach curves is confirmed by images from the area where the approach curves are taken [Fig. 4(b)]. The crater marks the location where an approach curve was measured. The force exerted for imaging is much smaller than the one applied during the measurement of the approach curves. (The top right corner is structureless due to a pixel saturation caused by the limitation in the dynamic range of the instrument implied by the need of high resolution for the approach curves.)

For Si and SiO_x, a larger bias voltage is needed to measure the point of contact. These high voltages will inevitably lead to the destruction of the thin conductive film on the probe tip upon contact. We can thus not reliably determine the point of contact for these samples.

In conclusion, we have presented measurements of oscillation amplitude and phase for a fiber-optical tip in a SNOM, approaching a sample surface in shear force feedback mode. This data is analyzed in terms of force and damping constants in an equivalent harmonic-oscillator model. The shear force interaction is shown to reflect different sample properties through fundamentally different properties of the force interaction: dissipative and/or elastic. The insulator and the semiconductor surface make the first contact through a dissipative interaction while the metal surface influences both the elastic and the dissipative channel. The similarities of the absolute values for the force constants indicate that the force channel largely reflects the properties of the probe tip. The dissipative channel is sample dependent and the interaction with respect to the force constant change depends on the specific sample. The microscopic processes underlying the shear force interaction are currently unknown. The dependence of the character of the shear force interaction on the electronic properties of the sample might be exploited to generate chemical or rather electronic contrast in the shear force AFM.

Acknowledgements

We acknowledge the financial support of the Deutsche Forschungsgemeinschaft through the collaborative research center SFB 290.

References

- [1] H. Heinzelmann, D.W. Pohl, *Appl. Phys. A* 59 (1994) 89.
- [2] D.W. Pohl, W. Denk, M. Lanz, *Appl. Phys. Lett.* 44 (1984) 651.
- [3] A. Harootunian, E. Betzig, M. Isaacson, A. Lewis, *Appl. Phys. Lett.* 49 (1986) 674.
- [4] R. Toledo-Crow, P.C. Yang, Y. Chen, M. Vaez-Iravani, *Appl. Phys. Lett.* 60 (1992) 2857.
- [5] E. Betzig, P.L. Finn, J.S. Weiner, *Appl. Phys. Lett.* 60 (1992) 2484.
- [6] K. Karrai, R.D. Grober, *Appl. Phys. Lett.* 66 (1995) 1842.
- [7] C.M. Mate, G.M. McClelland, R. Erlandsson, S. Chiang, *Phys. Rev. Lett.* 59 (1987) 1942.
- [8] P.K. Wei, W.S. Fann, *J. Appl. Phys.* 83 (1998) 3461.
- [9] P.K. Wei, W.S. Fann, *J. Appl. Phys.* 87 (2000) 2561.
- [10] J.U. Schmidt, H. Bergander, L.M. Eng, *Appl. Surf. Sci.* 157 (2000) 295.
- [11] M. Leuschner, M. Schüttler, H. Giessen, *J. Microscopy* 202 (2001) 176.
- [12] M. Schüttler, M. Leuschner, M. Lippitz, W.W. Rühle, H. Giessen, *Jap. J. Appl. Phys.* 40 (2001) 813.
- [13] J. Rychen, T. Ihn, P. Studerus, A. Herrmann, K. Ensslin, H.J. Hug, P.J.A. van Schendel, H.J. Güntherodt, *Rev. Sci. Instr.* 71 (2000) 1695.
- [14] K. Karrai, I. Tiemann, *Phys. Rev. B* 62 (2000) 13174.
- [15] O. Pfeiffer, R. Bennowitz, A. Baratoff, E. Meyer, P. Grütter, *Phys. Rev. B* 65 (2002) 161403.
- [16] B.C. Stipe, H.J. Mamin, T.D. Stowe, T.W. Kenny, D. Rugar, *Phys. Rev. Lett.* 87 (2001) 096801.
- [17] H.J. Mamin, D. Rugar, *Appl. Phys. Lett.* 79 (2001) 3359.
- [18] I. Dorofeyev, H. Fuchs, G. Wenning, B. Gotsman, *Phys. Rev. Lett.* 83 (1999) 2402.
- [19] A.I. Volokitin, B.N.J. Persson, *Phys. Rev. Lett.* 91 (2003) 106101.
- [20] M. Lippitz, M. Schüttler, H. Gießen, M. Born, W.W. Rühle, *J. Appl. Phys.* 86 (1999) 100.
- [21] F.J. Giessibl, *Appl. Phys. Lett.* 73 (1998) 3956.
- [22] P.P. Ong, *Physics Education* 37 (2002) 540.
- [23] D. Sarid, in: M. Lapp, H. Stark (Eds.), *Scanning Force Microscopy*, Oxford University Press, Oxford, 1991, p. 1.
- [24] David R. Lide (Ed.), *CRC Handbook of Chemistry and Physics*, CRC Press, Boca Raton, 2000.
- [25] P. Hoffmann, B. Dutoit, R.-P. Salathé, *Ultramicroscopy* 61 (1995) 165.